IL-37 suppresses macrophage ferroptosis to attenuate diabetic atherosclerosis via the NRF2 pathway

JINMEI XU[1*], XU HAN[2*], NAN XIA[1*], QINGSONG ZHAO[1] and ZHIFENG CHENG[1]

[1]Department of Endocrinology, Fourth Affiliated Hospital of Harbin Medical University, Harbin, Heilongjiang 150001;
[2]Medical Laboratory, Harbin Medical University, Daqing, Heilongjiang 163001, P.R. China

Abstract. IL-37 is a newly discovered inflammatory factor. However, the protective effect and underlying mechanisms of IL-37 on atherosclerosis remain unclear. In the present study, IL-37 was used for intraperitoneal injection in diabetic ApoE$^{-/-}$ mice caused by streptozotocin. High glucose (HG)/ox-LDL was used to stimulate THP-1 original macrophage followed by IL-37 pretreatment *in vitro*. The atheromatous plaque area, oxidative stress and inflammation levels in ApoE$^{-/-}$ mice were evaluated, and the level of macrophage ferroptosis was detected *in vivo* and *in vitro*. It was identified that IL-37 treatment significantly decreased plaque area in diabetic ApoE$^{-/-}$ mice. IL-37 not only improved blood lipid levels in mice, but also reduced serum levels of inflammatory factors including IL-1β and IL-18. Furthermore, IL-37 increased GPX4 and nuclear factor erythroid 2-related factor 2 (NRF2) in the aorta of diabetic mice. *In vitro* experiment revealed that IL-37 inhibited HG/ox-LDL-induced ferroptosis in macrophages, as evidenced by improved cell membrane oxidation, reduced malondialdehyde production and increased GPX4 expression. Moreover, it was also found that IL-37 enhanced the nuclear translocation of NRF2 in macrophages, while ML385, a specific NRF2 inhibitor, significantly attenuated the protective effect of IL-37 on macrophage ferroptosis caused by HG/ox-LDL. In conclusion, IL-37 suppressed macrophage ferroptosis to attenuate atherosclerosis progression via activating the NRF2 pathway.

Correspondence to: Dr Zhifeng Cheng, Department of Endocrinology, Fourth Affiliated Hospital of Harbin Medical University, 37 Yiyuan Street, Nangang, Harbin, Heilongjiang 150001, P.R. China
E-mail: 2020021033@hrbmu.edu.cn

*Contributed equally

Introduction

Atherosclerosis is one of the most common pathological mechanisms of cardiovascular diseases. Increasing evidence suggested that patients with diabetes have a significantly increased risk of atherosclerosis (1,2). Even though antiplatelet and lipid-lowering treatments now significantly improve the prognosis of patients with atherosclerosis, there remains a residual cardiovascular risk in certain patients, particularly those with diabetes. Therefore, there is an urgent need to find new potential targets for intervention against diabetic atherosclerosis.

There are increasing evidence demonstrated that inflammation is a key factor in the development of atherosclerosis (3). The CANTONS study noted that anti-inflammatory therapy targeting IL-1β may provide a limited reduction in the incidence of major adverse cardiovascular events in patients with acute myocardial infarction (4). In addition, interventions with IL-6 and NLRP3 inflammasome have also been found to reduce the incidence of atherosclerosis and complications. All of these data illustrated that targeting inflammatory pathways may be an effective intervention for atherosclerosis treatment (5,6). In addition to classical inflammatory factors, including IL-1β, TNF-α and IL-8, an increasing number of novel inflammatory factors are being identified due to their cardiovascular protective effects (7). IL-37 is a newly identified anti-inflammatory factor; it was found that IL-37 is significantly elevated in monocytes as well as in peripheral blood in patients with coronary artery disease and acute myocardial infarction (8,9). Moreover, IL-37 levels have also been shown to be strongly associated with the long-term prognosis of patients with acute myocardial infarction and acute stroke (10-13). Furthermore, it was also reported that overexpression of IL-37 significantly increases plaque instability in ApoE$^{-/-}$ mice (14). Furthermore, *in vitro* experiments demonstrated that IL-37 attenuated atherosclerosis by suppressing T cell activation, inducing the response of regulatory T cells and inhibiting vascular calcification (11,15-17). However, to the best of our knowledge, the effect and underlying mechanism of IL-37 on diabetic atherosclerosis remains unclear.

Ferroptosis is a form of programmed death characterized by lipid oxidation in the cell membrane. There is growing evidence that ferroptosis is extensively involved in the development and progression of atherosclerosis. It was reported that high levels

of uric acid promote the progression of atherosclerosis by increasing levels of oxidative stress and enhancing ferroptosis of macrophages (18). The use of a ferroptosis-specific inhibitor, Fer-1, has also been found to be effective in inhibiting the progression of atherosclerosis (19,20). Glutathione peroxidase 4 (GPX4), is mainly responsible for regulating glutathione synthesis in cells. When the expression of GPX4 is inhibited in cells, glutathione synthesis in cells becomes dysfunctional, which results in ferroptosis (21-23). Thus, the decrease of GPX4 was also regarded as the marker of ferroptosis (23). Several studies have revealed that IL-37 has a potent ability to scavenge oxygen radicals (8,11). However, whether IL-37 has a protective effect on ferroptosis of macrophages and the related mechanism remains unclear.

In the present study, the protective effect of IL-37 on diabetic atherosclerosis was confirmed; it was also found that IL-37 may attenuate the progression of atherosclerosis by suppressing ferroptosis of macrophages. The present study provided new evidence that IL-37 protects against atherosclerosis.

Materials and methods

Animal model. The present experiment was approved (approval no. SYDW2020-251) by the Ethics Committee of the Fourth Affiliated Hospital of Harbin Medical University (Harbin, China). The mice were housed in the animal center of the Second Affiliated Hospital of Harbin Medical University ($22\pm2°C$, $55\pm5\%$ relative humidity with a 12/12-h light/dark cycle). The mice were granted free access to food and water. Male ApoE$^{-/-}$ mice (8-week-old, 20-25 g) were randomly divided into two groups of 10 mice each. According to a previous study (24), a diabetes model was constructed using streptozotocin (STZ) intraperitoneal injection (50 mg/kg/day for five consecutive days) after 4 weeks of feeding using a high-fat diet. ApoE$^{-/-}$ mice with continuous blood glucose >15 mM were used as a model of diabetes. The mice were all administered a high-fat diet and divided into STZ/HD and IL-37 groups. Saline and IL-37 were administered intraperitoneally (1 μg/week), respectively (15). After 12 weeks, all animals were anesthetized with an intraperitoneal injection of sodium pentobarbital (35 mg/kg body weight) and then euthanized by cervical dislocation; serum and vascular tissue were collected.

Cell culture. THP-1 cells were cultured in RPMI-1640 medium (Gibco; Thermo Fisher Scientific, Inc.) with 10% fetal bovine serum (Gibco; Thermo Fisher Scientific, Inc.) and passaged once every 2-3 days. A total of 100 nM Phorbol-12-Myristate-13-Acetate was used to treat THP-1 cells for 48 h to induce into macrophages. Macrophages were divided into four groups: i) Control group (DMSO), ii) high glucose (HG)/ox-LDL (100 ng/ml ox-LDL, 25 mM glucose for 24 h), iii) IL-37/HG/ox-LDL (30 μM IL-37 for 0.5 h, 100 ng/ml ox-LDL, 25 mM glucose for 24 h) and iv) ML385 group (5 μM ML385 for 0.5 h, 30 μM IL-37 for 0.5 h, 100 ng/ml ox-LDL, 25 mM glucose for 24 h).

Western blot analysis. Macrophages and mouse aortic tissue were used to extract protein lysates using RIPA (Beyotime Institute of Biotechnology). Protein concentration was measured using a BCA kit (Beyotime Institute of Biotechnology). Protein (20 μg/lane) was separated by 10% sodium dodecyl sulfate-polyacrylamide gel electrophoresis and transferred onto polyvinylidene fluoride membranes (MilliporeSigma) using a semidry transblot apparatus (Bio-Rad Laboratories, Inc.). Next, the polyvinylidene fluoride membranes were blocked using 5% skimmed milk at room temperature for 60 min and the membrane was washed 3 times with PBS for 10 min each. PVDF membranes were incubated with the primary antibody (anti-GPX4 antibody: cat. no. 59735; 1:1,000; CST Biological Reagents Co., Ltd.; anti-NRF2 antibody: cat. no. 12721; 1:1,000; CST Biological Reagents Co., Ltd.; anti-Histone H3 antibody: cat. no. 14499; 1:2,000; CST Biological Reagents Co., Ltd.; anti-β-actin: cat. no. AC006; 1:1,000; ABclonal Biotech Co., Ltd.) overnight at 4°C. The next day, three washes using PBS for 10 min each followed. Subsequently, the membranes were incubated for 1 h at room temperature using HRP-labeled Goat Anti-Rabbit IgG (cat. no. A0208; 1:10,000; Beyotime Institute of Biotechnology). The immuno-reactive bands were detected by chemiluminescence methods and visualized using the Luminescent Imaging Workstation (Tanon Science and Technology Co., Ltd.). The relative intensities of the bands were measured and analyzed using the ImageJ software v.1.4 (National Institutes of Health).

Immunofluorescence staining. To detect nuclear translocation of nuclear factor erythroid 2-related factor 2 (NRF2), THP-1 macrophages were treated with 4% paraformaldehyde for 10 min at room temperature, washed three times with PBS and then treated with 0.3% Triton for 5 min at room temperature to disrupt the cell membrane. The cells were then washed three times with PBS at room temperature and 5% bovine serum albumin was added followed by incubation for 60 min to reduce non-specific staining at room temperature. The macrophages were incubated overnight at 4°C with primary antibody against NRF2 (cat. no. 12721; 1:100; CST Biological Reagents Co., Ltd.). Next, the macrophages were washed with PBS and incubated for 60 min at room temperature in the dark with a fluorescent Goat Anti-Rabbit secondary antibody (cat. no. ab150077; 1:400; Abcam). The macrophages were observed and images were captured on a confocal laser microscope (LSM 800) at x200 magnification.

Malondialdehyde (MDA), reduced glutathione (GSH) and superoxide dismutase (SOD measurement). The lysates of macrophages were extracted according to the manufacturer's instructions, and the levels of MDA (cat. no. S0131S; Beyotime Institute of Biotechnology), GSH (cat. no. S0053; Beyotime Institute of Biotechnology) and SOD (cat. no. S0101S; Beyotime Institute of Biotechnology) were measured using kits, and the absorbance (MDA, 532 nm; GSH, 412 nm; SOD, 450 nm) was analyzed using an enzyme marker.

C11 BODIPY measurement. According to the manufacturer's instructions, $1x10^6$ cells/ml were treated and digested using trypsin. PBA wash was performed 3 times and the level of lipid oxidation in the cell membrane was detected using C11 BODIPY (Thermo Fisher Scientific, Inc.) staining reagent (1:1,000 with PBS). After incubation for 30 min at room

temperature and protected from light, PBS was washed. The absorbance was detected using flow cytometry (581/591).

Cell viability assays. Macrophages were cultured in 96 well plates with 10,000 cells per well. The Cell Counting Kit-8 (CCK-8) (Beyotime Institute of Biotechnology) assays were performed according to the manufacturer's instructions. Briefly, after preparing the experimental groups and performing the cell treatments, the CCK-8 working solution was diluted 10-fold and 100 μl was removed and added to 96-well plates. The plates were placed in an incubator (37˚C, 60 min) to allow the reaction to occur. After the incubation, absorbance was measured at 450 nm using a microplate spectrophotometer (Tecan Group, Ltd.).

Lactate dehydrogenase (LDH) assays. Macrophages were cultured in 96 well plates with 10,000 cells per well. According to the LDH Assay Kit (cat. no. C0016; Beyotime Institute of Biotechnology) instructions, the cell culture plates after drug stimulation were centrifuged at 400 x g for 5 min using a multi-well plate centrifuge at room temperature. The LDH-releasing reagent provided in the kit was diluted 10-fold with PBS and mixed well. The cell supernatant was aspirated and 150 μl of the diluted LDH-releasing reagent was added to each cell sample. The plates were shaken to assure the LDH-releasing reagent in each well was mixed well. The plates were then incubated (37˚C) for 1 h. The cell culture plates were subsequently centrifuged for 5 min at room temperature at 400 x g in a multi-well plate centrifuge. The supernatant (120 μl) was collected from each well and separately added to the corresponding wells of a new 96-well plate. Thereafter the absorbance was measured at 490 nm.

Hoechst/propidium iodide (PI) staining. Cells were seeded into 24-well plates with 50,000 cells per well. After the cells were treated according to the experimental design, the cells were washed three times with PBS. Then, 5 μl Hoechst staining solution was added, followed by 5 μl PI stain. The cells were mixed and incubated in an ice bath at 4˚C for 20-30 min. The cells were carefully washed three times with PBS and an anti-fluorescence quenching agent (Beyotime Institute of Biotechnology) was added. Cells were observed under a fluorescence microscope at x200 magnification and images captured. To calculate the percentage of PI-positive cells, the number of PI-positive cells was divided by the number of Hoechst-positive cells. Three random fields were chosen for this calculation.

HE staining. The artery tissue from mice were fixed in 4% paraformaldehyde at 4˚C and processed for paraffin or optimal cutting temperature embedding. Embedded tissues were sliced to 8 μM, then HE staining were performed following the manufacturer's instructions (cat. no. C0105S; Beyotime Institute of Biotechnology). Eosin was used for 5 min at room temperature and hematoxylin for 5 min at room temperature.

Statistical analysis. All experiments were independently repeated more than three times. All statistical analyses were performed using the GraphPad Prism 8.0 software (Dotmatics) and were presented as the mean ± standard deviations (SDs).

Statistical differences among groups were determined using unpaired Student's t-test or by one-way ANOVA followed by Tukey's post hoc analysis. Each experiment was repeated at least three times, and differences with $P<0.05$ were considered statistically significant.

Results

IL-37 improves the decreased cell viability in macrophages induced by HG/ox-LDL. To determine the working concentration of IL-37, THP-1 derived macrophages were treated using 5, 10, 20, 30 and 40 μM of IL-37. Cell viability was assayed after 24 h. It was found that IL-37 at <30 μM did not exhibit significant cytostatic effects on macrophages (Fig. 1A). To mimic the HG and high fat environment in diabetic mice, HG (25 mM) and ox-LDL (100 ng/ml) were combined to stimulate macrophages. CCK-8 assay demonstrated that IL-37 treatment significantly improved that decrease of cell viability in macrophages induced by HG/ox-LDL (Fig. 1B). Oxidative damage to cell membranes is considered to be a key feature of ferroptosis (18). LDH assay and Hoechst-PI staining were used to detect the function of the cell membrane. A significant increase was found in PI-positive cells in the HG/ox-LDL group and a significant increase in LDH levels in the supernatant. However, these changes were attenuated by IL-37 treatment (Fig. 1C-E).

IL-37 suppresses macrophage ferroptosis by improving oxidative stress. Western blot analysis was used to evaluate the expression of GPX4, the marker of ferroptosis. The results demonstrated that GPX4 was significantly decreased in HG/ox-LDL group, while IL-37 treatment significantly increased the GPX4 level (Fig. 2A and B). Increased cell membrane phospholipid oxidation and MDA levels are key events in ferroptosis (18). C11 staining was next used to evaluate the oxidation of macrophage cell membranes, and it was found that IL-37 almost reversed the cell membrane oxidation caused by HG/ox-LD treatment (Fig. 2C and D). Moreover, IL-37 also decreased the elevated MDA level in the HG/ox-LDL group (Fig. 2E). The GSH level and SOD activity in macrophages were also determined. These results demonstrated that IL-37 treatment significantly increased the GSH level and SOD activity in the HG/ox-LDL group (Fig. 2F and G). These results revealed that IL-37 suppressed macrophage ferroptosis by improving oxidative stress. Furthermore, it was also found that IL-37 inhibited HG/ox-LDL-induced ferroptosis in mouse bone marrow-derived macrophages (Fig. S1).

IL-37 promotes NRF2 activation via enhancing NRF2 nuclear translocation. NRF2 acts as one of the most common cytosolic transcription factors regulating oxidative stress metabolism and inflammation. Under physiological conditions, NRF2 is located in the cell nucleus. It is mainly responsible for regulating the transcription of antioxidant proteins (18). From the immunofluorescence staining, it was observed that HG/ox-LDL significantly inhibited NRF2 nuclear translocation, while IL-37 attenuated this change (Fig. 3A and B). Furthermore, cellular nuclear proteins were extracted and western blot analysis was used to detect NRF2
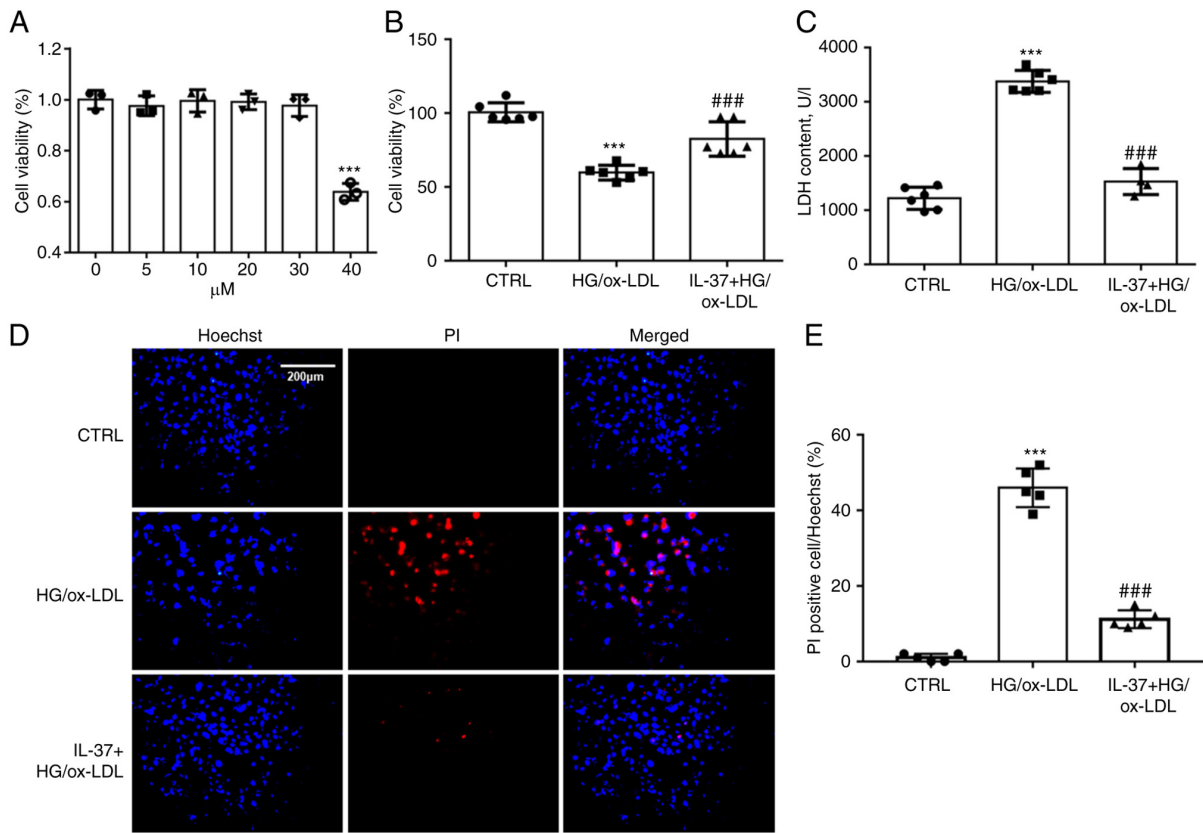
Figure 1. IL-37 ameliorates the decrease in cell viability caused by HG/ox-LDL. (A) CCK-8 assay, the macrophages were treated with 0, 5, 10, 20, 30 and 40 μM IL-37 for 24 h. The macrophages were divided into three groups: i) CTRL group; ii) HG/ox-LDL group: The macrophages were treated with 100 ng/ml ox-LDL and 25 mM glucose for 24 h; iii) IL-37 group: 30 μM IL-37 for 0.5 h, 100 ng/ml ox-LDL, 25 mM glucose for 24 h. (B) CCK-8 assay. (C) LDH assay. (D and E) Hoechst-PI staining. ***$P<0.001$ vs. control group and ###$P<0.001$ vs. HG/ox-LDL. Each dot represents a biological repetition. HG, high glucose; CCK-8, Cell Counting Kit-8; LDH, lactate dehydrogenase.
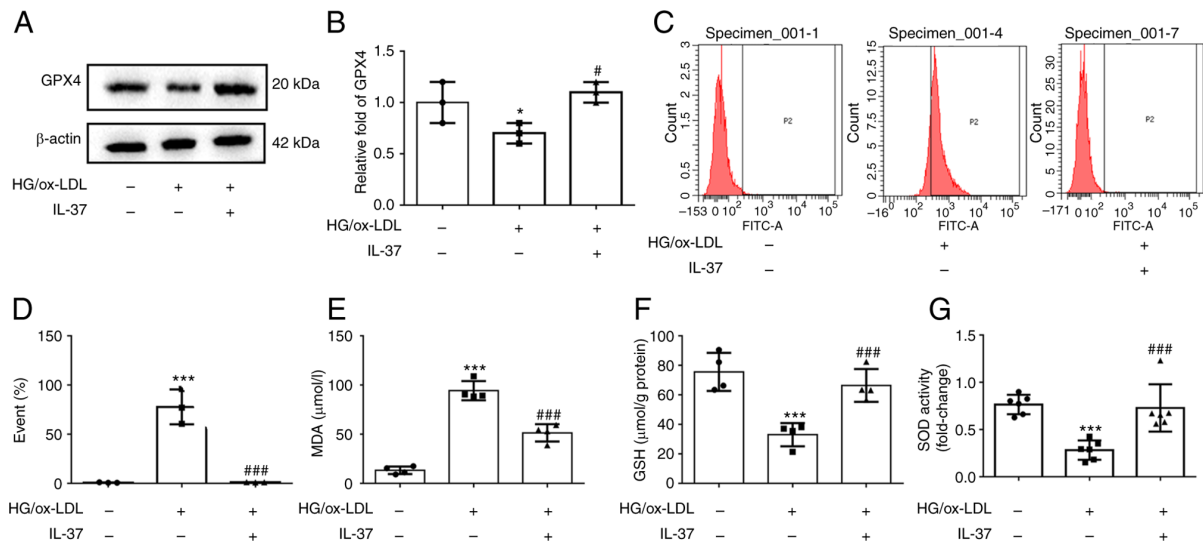

Figure 2. IL-37 inhibits ferroptosis of macrophages and oxidative stress caused by HG/ox-LDL. The macrophages were divided into three groups: i) CTRL group; ii) HG/ox-LDL group: The macrophages were treated with 100 ng/ml ox-LDL and 25 mM glucose for 24 h; and iii) IL-37 group: 30 μM IL-37 for 0.5 h, 100 ng/ml ox-LDL, 25 mM glucose for 24 h. (A and B) Western blot analysis was used to analyze the protein level of GPX4. (C and D) C11 BODIPY staining was used to analyze lipid peroxidation levels of macrophage cell membranes in different groups. (E) MDA level in different group. (F) GSH level in different group. (G) SOD level in different group. *$P<0.05$ vs. control group, ***$P<0.001$ vs. control group and #$P<0.05$ vs. HG/ox-LDL, ###$P<0.001$ vs. HG/ox-LDL. Each dot represents a biological repetition. HG, high glucose; GPX4, glutathione peroxidase 4; MDA, malondialdehyde; GSH, reduced glutathione; SOD, superoxide dismutase.

levels. It was similarly found that NRF2 levels in the nucleus were significantly decreased in the HG/ox-LDL group and
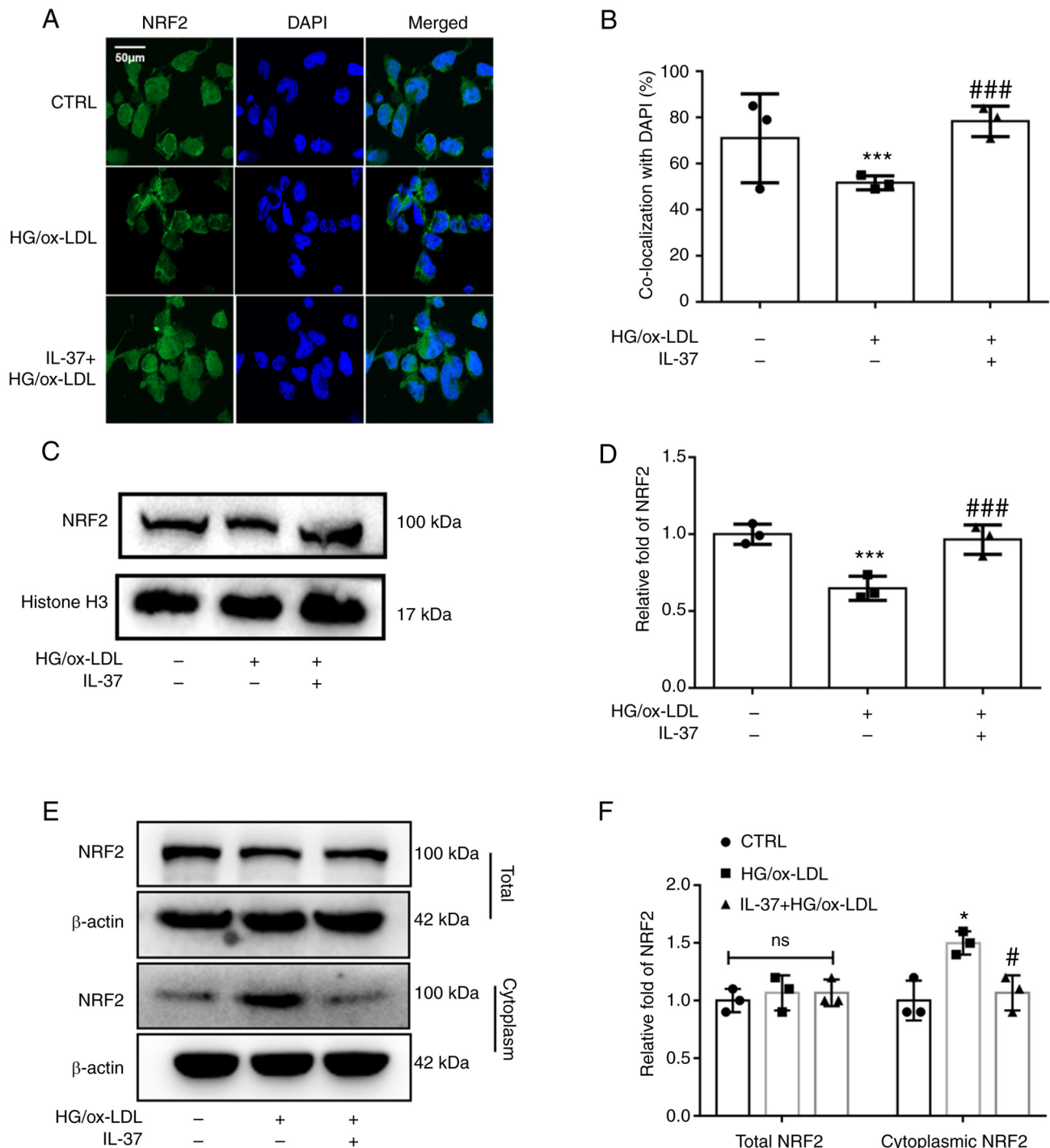
Figure 3. IL-37 enhances NRF2 nuclear translocation. The macrophages were divided into three groups: i) CTRL group; ii) HG/ox-LDL group: The macrophages were treated with 100 ng/ml ox-LDL and 25 mM glucose for 24 h; and iii) IL-37 group: 30 μM IL-37 for 0.5 h, 100 ng/ml ox-LDL, 25 mM glucose for 24 h. (A and B) Immunofluorescence was used to observe the level of NRF2 in the nuclei of different groups. (C and D) Macrophage nuclear proteins were extracted and western blotting was used to evaluate the level of NRF2 in the nucleus. (E and F) Macrophage total and cytoplasmic proteins were extracted and western blotting was used to evaluate the level of NRF2 in the nucleus. *P<0.05, ***P<0.001 vs. control group and #P<0.01, ###P<0.001 vs. HG/ox-LDL. Each dot represents a biological repetition. NRF2, nuclear factor erythroid 2-related factor 2; HG, high glucose.

significantly increased after IL-37 treatment (Fig. 3C and D). In addition, it was revealed that IL-37 did not affect the total NRF2 content in macrophages, but reduced the level of NRF2 in the cytoplasm of macrophages compared with the HG/ox-LDL group (Fig. 3E and F). These results suggested that IL-37 promotes NRF2 transfer from the cytoplasm to the nucleus.

IL-37 inhibits ferroptosis of macrophages by activating the NRF2 pathway. To further confirm if IL-37 inhibits ferroptosis of macrophages caused by HG/ox-LDL by promoting NRF2 activation, ML385 (a specific inhibitor of NRF2) was used to pretreat macrophages. Firstly, it was found that ML385 attenuated the protective effect of IL-37 against macrophage viability (Fig. 4A). Secondly, after ML385 pretreatment, the LDH level in
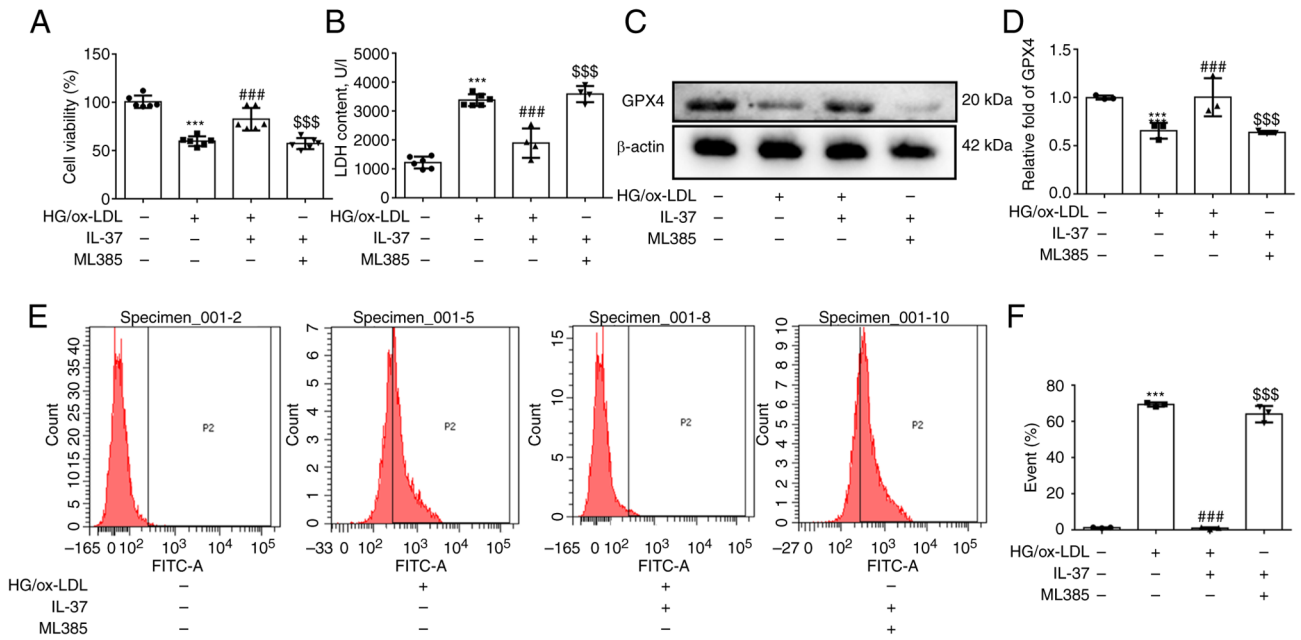
Figure 4. ML385 abrogates the ferroptosis protection of IL-37. The macrophages were divided into four groups: i) CTRL group; ii) HG/ox-LDL group: The macrophages were treated with 100 ng/ml ox-LDL and 25 mM glucose for 24 h; iii) IL-37 group: 30 μM IL-37 for 0.5 h, 100 ng/ml ox-LDL, 25 mM glucose for 24 h; and iv) ML385 group: 5 μM ML385 for 0.5 h, 30 μM IL-37 for 0.5 h, 100 ng/ml ox-LDL, 25 mM glucose for 24 h. (A) Cell Counting Kit-8 assay was used to evaluate the cell viability in different groups. (B) LDH assay was used to analyze the LDH content in cell supernatant. (C and D) Western blotting was used to detected the level of GPX4 in different groups. (E and F) C11 BODIPY staining was used to analyze lipid peroxidation levels of macrophage cell membranes in different groups. ***P<0.001 vs. control group, ###P<0.001 vs. HG/ox-LDL and $$$P<0.001 vs. IL-37/HG/ox-LDL. Each dot represents a biological repetition. HG, high glucose; LDH, lactate dehydrogenase; GPX4, glutathione peroxidase 4.
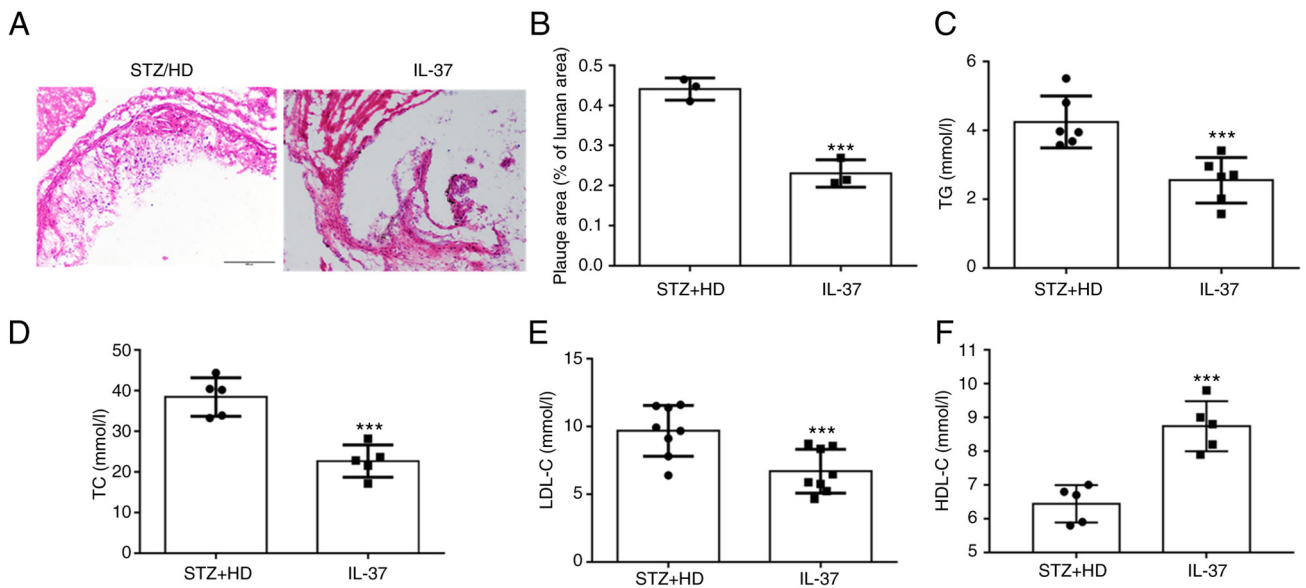

Figure 5. IL-37 suppresses the development of atherosclerosis. Diabetic ApoE^{-/-} mice were divided into two groups: i) STZ/HD group: The mice were fed with high-fat feed for 12 weeks and received the same amount of saline intraperitoneally; and ii) IL-37 group: The mice were fed with high-fat feed for 12 weeks and received IL-37 intraperitoneally (1 μg/week). (A and B) H&E staining was used to evaluate the aortic root plaque area in mice. (C) Serum TG level. (D) Serum TC level. (E) Serum LDL-C level. (F) Serum HDL-C level. ***P<0.001 vs. STZ/HD group. Each dot represents a biological repetition. STZ, streptozotocin; TG, triglycerides; TC, total cholesterol.

IL-37 group was also significantly increased (Fig. 4B). Thirdly, it was demonstrated that ML385 significantly decreased the GPX4 level (Fig. 4C and D). Finally, the inhibitory effect of IL-37 on cell membrane phospholipid oxidation was completely abolished by ML385 (Fig. 4E and F). Furthermore, the promotion of NRF2 nuclear translocation by IL-37 was significantly reversed by ML385 (Fig. S2). Overall, these results strongly confirmed that IL-37 inhibits ferroptosis of macrophage macrophages through activation of the NRF2 pathway.

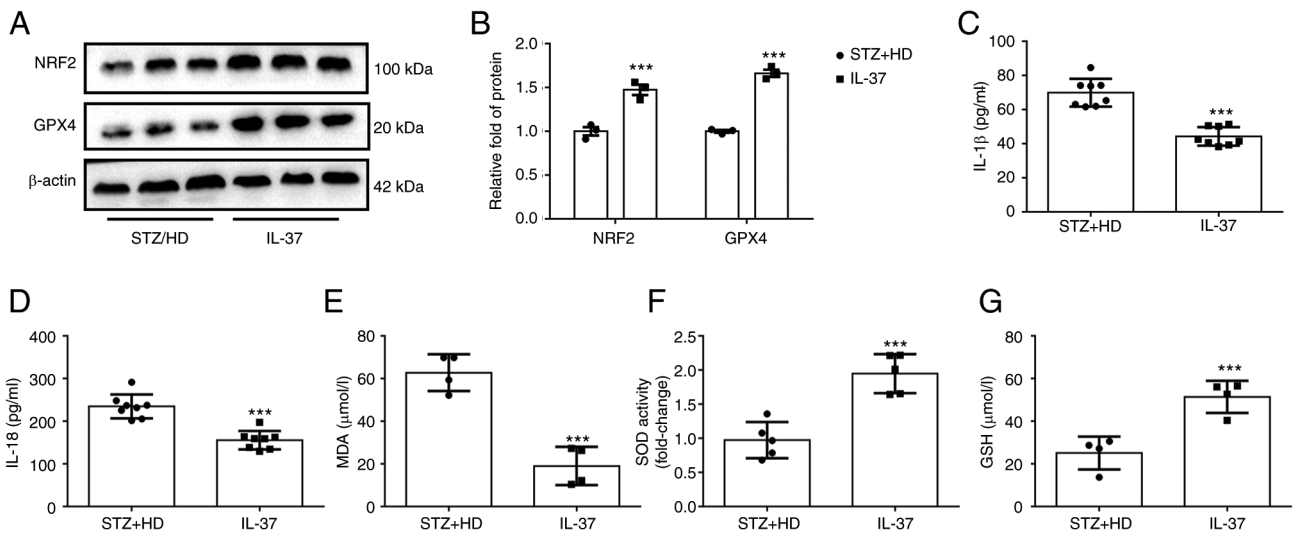*IL-37 attenuates atherosclerosis progression in diabetic ApoE^{-/-} mice.* In the current study, STZ was used to construct

Figure 6. IL-37 improves oxidative stress in diabetic ApoE-/- mice. Diabetic ApoE-/- mice were divided into two groups: i) STZ/HD group: The mice were fed with high-fat feed for 12 weeks and received the same amount of saline intraperitoneally; and ii) IL-37 group: The mice were fed with high-fat feed for 12 weeks and received IL-37 intraperitoneally (1 μg/week). (A and B) Western blotting was used to analyze the level of GPX4 and NRF2 in mice aortic lysate. (C) Serum IL-1β level in different groups. (D) Serum IL-18 level in different groups. (E) Serum MDA level in different groups. (F) Serum SOD level in different groups. (G) Serum GSH level in different groups. ***$P<0.001$ vs. STZ/HD group. Each dot represents a biological repetition. STZ, streptozotocin; GPX4, glutathione peroxidase 4; NRF2, nuclear factor erythroid 2-related factor 2; MDA, malondialdehyde; SOD, superoxide dismutase; GSH, reduced glutathione.

a model of diabetes. These mice were administered high-fat feeding for 12 weeks. For H&E staining at the aortic sinus, it was observed that IL-37 treatment significantly reduced the plaque area (Fig. 5A and B). Moreover, lipid levels were evaluated in mice and it was found that IL-37 treatment significantly reduced triglycerides, total cholesterol and LDL-C levels (Fig. 5C-E). In addition, IL-37 increased the level of HDL-C in HD/STZ group (Fig. 5D). These data indicated that IL-37 effectively inhibited the progression of atherosclerosis and improved blood lipid levels in diabetic ApoE$^{-/-}$ mice.

IL-37 inhibits ferroptosis of macrophages, oxidative stress and inflammatory response in diabetic ApoE$^{-/-}$ mice. To further confirm the protective effect of IL-37 against ferroptosis *in vivo*, lysate was extracted from mouse aorta and the levels of NRF2 and GPX4 were detected using western blot analysis. The results revealed that the protein levels of GPX4 and NRF2 were significantly increased in IL-37-treated mice (Fig. 6A and B). Furthermore, the IL-18 and IL-1β levels in serum were detected and it was found that IL-37 treatment significantly decreased the IL-18 and IL-1β levels in diabetic ApoE-/- mice (Fig. 6C and D). Lastly, the serum levels of MDA, GSH and SOD in mice were evaluated. The data demonstrated that IL-37 treatment increased the GSH level, enhanced SOD activity and decreased the MDA level in diabetic ApoE$^{-/-}$ mice (Fig. 6E-G). These *in vivo* results confirmed that IL-37 has the ability to inhibit ferroptosis and inflammation and improve oxidative stress.

Discussion

The main findings of the present study are as follows: i) IL-37 inhibited ferroptosis in macrophages caused by HG/ox-LDL; ii) IL-37 inhibits macrophage ferroptosis by activating the NRF2 pathway; and iii) IL-37 attenuated diabetic atherosclerosis by inhibiting macrophage ferroptosis. The present results

suggested that IL-37 may serve as a new potential intervention target for atherosclerosis therapy.

Ferroptosis is a newly discovered mode of programmed cell death. In recent years, studies from autopsies and animal experiments have reported that ferroptosis is extensively involved in the development and progression of atherosclerosis (25-27). Evidence from clinical researches suggested that HMOX1, a key gene of ferroptosis, is strongly associated with the prognosis of patients with atherosclerosis (28). Clinical data also suggested that genes for ferroptosis can be used as biomarkers of atherosclerosis (29). It was reported that erythroid lineage Jak2V617F expression contributes to the progression of atherosclerosis by enhancing macrophage ferroptosis (30). Moreover, it was also found that inhibition of ferroptosis can effectively improve atherosclerosis. Yang *et al* (31) reported that prenyl-diphosphate synthase subunits suppressed the of endothelial cells ferroptosis in atherosclerosis by activating the NRF2 pathway. A previous study (32) showed that Fer-1 inhibits atherosclerosis progression in ApoE$^{-/-}$ mice by suppressing ferroptosis in endothelial cells. These results all suggested that either macrophage or endothelial cell ferroptosis is involved in the development of atherosclerosis; thus ferroptosis may be a potential target for intervention in atherosclerosis. In the present study, both *in vivo* and *in vitro* evidence found that IL-37 inhibits ferroptosis in macrophages caused by HG/ox-LDL. It was also revealed that IL-37 could improve oxidative stress caused by HG/ox-LDL. Previous studies also demonstrated that IL-37 reduced HG-induced inflammation and oxidative stress. It was previously reported (33) that IL-37 could ameliorate oxidative damage in epithelial cells in diabetic kidney injury via the STAT3 pathway. Furthermore, it was found that the level of IL-37 was negatively correlated with oxidative stress in patients with Hashimoto's thyroiditis, which also suggests that IL-37 has an inhibitory effect on oxidative stress (34). The results of the present study found

that IL-37 also has a broad antioxidant capacity in atherosclerosis, and in addition, it was further identified that IL-37 may attenuate ferroptosis of macrophages by ameliorating oxidative stress. In addition, it was found that IL-37 improved diabetic atherosclerosis, and IL-37 improved macrophage ferroptosis in both *in vivo* and *in vitro* experiments. However, this does not directly indicate that IL-37 improves diabetic atherosclerosis by inhibiting ferroptosis in macrophages. Previous studies have identified the role of macrophage iron death in promoting atherosclerosis (18,30,35). Furthermore, it was reported that the ferroptosis inhibitor, Fer-1, can significantly improve atherosclerosis (32). These evidence directly confirm that macrophage ferroptosis promotes atherosclerosis, which also supports the present conclusion to certain extent. On the other hand, IL-37 may improve atherosclerosis by inhibiting macrophages in other ways, such as inhibiting apoptosis of macrophages and promoting autophagy. Further experiments are needed to confirm this.

As a newly discovered inflammatory factor, the anti-inflammatory effect of IL-37 is gradually being investigated. Several studies demonstrated that IL-37 has potential protective effects against inflammatory diseases, including colitis and gastritis (36-38). Furthermore, it was also reported that IL-37 improved the function of plasma dendritic cells in patients with acute coronary syndrome (11). The inflammatory response is one of the key mechanisms of diabetic atherosclerosis. However, no previous studies have focused on the role of IL-37 on the level of inflammation in diabetic atherosclerotic mice. The current data revealed that the levels of classical pro-inflammatory factors, IL-1β and IL-18, in peripheral blood were significantly decreased in diabetic atherosclerotic mice after continuous intraperitoneal injection of IL-37. The results of the present study confirmed the potent anti-inflammatory ability of IL-37 in atherosclerosis, which is consistent with the phenomenon found in clinical patients. Thus, anti-inflammation may be one of the potential mechanisms by which IL-37 exerts athero-protective effects. However, the mechanism of IL-37 inhibition of inflammation in HG/ox-LDL-treated macrophages was not further investigated. This is one of the limitations to the current study. Previous studies have confirmed that IL-37 is a potential inhibitor of P65 and may exert anti-inflammatory effects by inhibiting the phosphorylation and nuclear translocation of P65 (39-41). P65 activation has also been suggested as a key mechanism for increased inflammation levels in diabetic atherosclerotic mice (42,43). Therefore, further studies are needed to focus on the mechanisms underlying the role of IL-37 on P65 activation in diabetic atherosclerotic mice.

NRF2 is a classical transcription factor. NRF2 regulates proteins of inflammation and oxidative stress and has received a lot of attention for this reason. Under physiological conditions, NRF2 is localized in the nucleus and is responsible for binding the promoter of the antioxidant protein progenitor to maintain oxidative stress homeostasis in the cell. In the present study, it was found that macrophages treated with HG/ox-LDL showed a significant decrease in NRF2 levels in the nucleus and a significant downregulation of GPX4, GSH and SOD levels, compared with the normal group. IL-37 treatment not only increased the expression of NRF2 in the nucleus, but also upregulated the levels of GPX4, GSH and

SOD. However, ML383 abolished these changes. These results provide strong evidence that IL-37 inhibits macrophage ferroptosis by activating the NRF2 pathway. As a classical transcription factor, a large number of studies have reported that the transfer of NRF2 to the nucleus is the key to the biological function of NRF2 (18,28,44). It was reported that lycopene ameliorates DEHP exposure-induced renal pyroptosis through enhancing NRF2 nuclear translocation (45). In the present study, the content of NRF2 was evaluated in the nucleus of ML385 treatment, and it was found that the nuclear translocation of NRF2 caused by IL-37 treatment was significantly inhibited by ML385. Furthermore, ML385 inhibits the activity of NRF2, which is activated by IL-37. Therefore, it was hypothesized that IL-37 may activate NRF2 pathway by promoting NRF2.

It was reported that NRF2 plays a critical role in mitigating lipid peroxidation and ferroptosis (46). It was found that exogenous activation of NRF2 inhibits acute lung injury due to intestinal ischemia via SLC7A11/HO-1 (47). Furthermore, inhibition of NRF2 has been reported to exacerbate acute myocardial injury caused by doxorubicin (48). These results are consistent with the findings of the present study. Moreover, it was observed that IL-37 increased NRF2 expression of IL-37 in diabetic mice, but *in vitro* experiment found that IL-37 had no effect on total NRF2 level in macrophages. This has been previously reported, as Luo *et al* (49) demonstrated that after ox-LDL treatment of macrophages, the total protein level of NRF2 did not change and NRF2 was reduced in the nucleus, and quercetin treatment could inhibit this phenomenon. However, in high-fat fed ApoE$^{-/-}$ mice, total vascular NRF2 decreased and quercetin increased total vascular NRF2 expression. At the cellular level, there may be feedback regulation in macrophages treated with HG/ox-LDL, resulting in unchanged NRF2 level and only decreased NRF2 level in the nucleus. Then, in ApoE$^{-/-}$ mice, atherosclerotic plaques had occurred, and the feedback regulatory effect of macrophages was weakened or lost, which led to a decrease in NRF2 expression, but IL-37 could ameliorate this phenomenon.

There are certain limitations to the present study. It was only found that IL-37 improved diabetic atherosclerosis and that IL-37 improved macrophage ferroptosis. Nevertheless, this does not directly indicate that IL-37 improves diabetic atherosclerosis by inhibiting ferroptosis in macrophages. Macrophage-deletion mice are needed to further confirm that IL-37 inhibits ferroptosis in macrophages to protect atherosclerosis. Secondly, at the animal level, NrF2-deficient knockout mice confirmed that IL-37 improves ferroptosis in macrophages by activating NRF2.

In conclusion, it was identified that IL-37 suppresses ferroptosis of macrophages to attenuate atherosclerosis via activating the NRF2 pathway.

Availability of data and materials

The datasets used and/or analyzed during the current study are available from the corresponding author on reasonable request.

Authors' contributions

ZC developed the analysis plan and wrote the manuscript. QZ, JX, XH and NX performed the main experiments and data analysis. ZC and XJ confirm the authenticity of all the raw data. All authors contributed to manuscript revision, and have read and approved the final manuscript.

Ethics approval and consent to participate

The present experiment was approved (approval no. SYDW2020-251) by the Ethics Committee of the Fourth Affiliated Hospital of Harbin Medical University (Harbin, China).

Patient consent for publication

Not applicable.

Competing interests

The authors declare that they have no competing interests.

References

1. Lopez-Jimenez F, Almahmeed W, Bays H, Cuevas A, Di Angelantonio E, le Roux CW, Sattar N, Sun MC, Wittert G, Pinto FJ and Wilding JPH: Obesity and cardiovascular disease: mechanistic insights and management strategies. A joint position paper by the world heart federation and world obesity federation. Eur J Prev Cardiol 29: 2218-2237, 2022.
2. Boswell L, Serés-Noriega T, Mesa A, Perea V, Pané A, Viñals C, Blanco J, Giménez M, Vinagre I, Esmatjes E, et al: Carotid ultrasonography as a strategy to optimize cardiovascular risk management in type 1 diabetes: A cohort study. Acta Diabetol 59: 1563-1574, 2022.
3. Wang C, Liu C, Shi J, Li H, Jiang S, Zhao P, Zhang M, Du G, Fu S, Li S, et al: Nicotine exacerbates endothelial dysfunction and drives atherosclerosis via extracellular vesicle-miRNA. Cardiovasc Res 25: cvac140, 2022.
4. Everett BM, MacFadyen JG, Thuren T, Libby P, Glynn RJ and Ridker PM: Inhibition of interleukin-1β and reduction in atherothrombotic cardiovascular events in the cantos trial. J Am Coll Cardiol 76: 1660-1670, 2020.
5. Ferencik M, Mayrhofer T, Lu MT, Bittner DO, Emami H, Puchner SB, Meyersohn NM, Ivanov AV, Adami EC, Voora D, et al: Coronary atherosclerosis, cardiac troponin, and interleukin-6 in patients with chest pain: The PROMISE trial results. JACC Cardiovasc Imaging 15: 1427-1438, 2022.
6. Andreotti F, Maggioni AP, Campeggi A, Iervolino A, Scambia G and Massetti M: Anti-inflammatory therapy in ischaemic heart disease: From canakinumab to colchicine. Eur Heart J Supp 23: E13-E18, 2021.
7. Liberale L, Kraler S, Puspitasari YM, Bonetti NR, Akhmedov A, Ministrini S, Montecucco F, Marx N, Lehrke M, Hartmann NUK, et al: SGLT-2 inhibition by empagliflozin has no effect on experimental arterial thrombosis in a murine model of low-grade inflammation. Cardiovasc Res 22: cvac126, 2022.
8. Li H, Shen C, Chen B, Du J, Peng B, Wang W, Chi F, Dong X, Huang Z and Yang C: Interleukin-37 is increased in peripheral blood mononuclear cells of coronary heart disease patients and inhibits the inflammatory reaction. Mol Med Rep 21: 151-160, 2020.
9. Law CC, Puranik R, Fan J, Fei J, Hambly BD and Bao S: Clinical implications of IL-32, IL-34 and IL-37 in atherosclerosis: Speculative role in cardiovascular manifestations of COVID-19. Front Cardiovasc Med 8: 630767, 2021.
10. Zhang F, Zhu T, Li H, He Y, Zhang Y, Huang N, Zhang G, Li Y, Chang D and Li X: Plasma Interleukin-37 is elevated in acute ischemic stroke patients and probably associated with 3-month functional prognosis. Clin Interv Aging 15: 1285-1294, 2020.
11. Zhu R, Zhang F, Pan C, Yu K, Zhong Y and Zeng Q: Role of IL-37- and IL-37-treated dendritic cells in acute coronary syndrome. Oxid Med Cell Long 2021: 6454177, 2021.
12. Rafiei A, Ahmadi R, Kazemian S, Rahimzadeh-Fallah T, Mohammad-Rezaei M, Azadegan-Dehkordi F, Sanami S, Mirzaei Y, Aghaei F and Bagheri N: Serum levels of IL-37 and correlation with inflammatory cytokines and clinical outcomes in patients with coronary artery disease. J Invest Med 70: 1720-1727, 2022.
13. Liu K, Tang Q, Zhu X and Yang X: IL-37 increased in patients with acute coronary syndrome and associated with a worse clinical outcome after ST-segment elevation acute myocardial infarction. Clin Chim Acta 468: 140-144, 2017.
14. Liu J, Lin J, He S, Wu C, Wang B, Liu J, Duan Y, Liu T, Shan S, Yang K, et al: Transgenic overexpression of IL-37 protects against atherosclerosis and strengthens plaque stability. Cell Physiol Biochem 45: 1034-1050, 2018.
15. Ji Q, Meng K, Yu K, Huang S, Huang Y, Min X, Zhong Y, Wu B, Liu Y, Nie S, et al: Exogenous interleukin 37 ameliorates atherosclerosis via inducing the Treg response in ApoE-deficient mice. Sci Rep 7: 3310, 2017.
16. Chai M, Ji Q, Zhang H, Zhou Y, Yang Q, Zhou Y, Guo G, Liu W, Han W, Yang L, et al: The protective effect of interleukin-37 on vascular calcification and atherosclerosis in apolipoprotein e-deficient mice with diabetes. J Interferon Cytokine Res 35: 530-539, 2015.
17. Lotfy H, Moaaz M and Moaaz M: The novel role of IL-37 to enhance the anti-inflammatory response of regulatory T cells in patients with peripheral atherosclerosis. Vascular 28: 629-642, 2020.
18. Yu W, Liu W, Xie D, Wang Q, Xu C, Zhao H, Lv J, He F, Chen B, Yamamoto T, et al: High level of uric acid promotes atherosclerosis by targeting NRF2-mediated autophagy dysfunction and ferroptosis. Oxid Med Cell Longev 2022: 9304383, 2022.
19. Ouyang S, You J, Zhi C, Li P, Lin X, Tan X, Ma W, Li L and Xie W: Ferroptosis: The potential value target in atherosclerosis. Cell Death Dis 12: 782, 2021.
20. Hu H, Chen Y, Jing L, Zhai C and Shen L: The link between ferroptosis and cardiovascular diseases: A novel target for treatment. Front Cardiovasc Med 8: 710963, 2021.
21. Yu Y, Yan Y, Niu F, Wang Y, Chen X, Su G, Liu Y, Zhao X, Qian L, Liu P and Xiong Y: Ferroptosis: A cell death connecting oxidative stress, inflammation and cardiovascular diseases. Cell Death Disc 7: 193, 2021.
22. Duan JY, Lin X, Xu F, Shan SK, Guo B, Li FXZ, Wang Y, Zheng MH, Xu QS, Lei LM, et al: Ferroptosis and its potential role in metabolic diseases: A curse or revitalization? Front Cell Dev Biol 9: 701788, 2021.
23. Zhou Y, Zhou H, Hua L, Hou C, Jia Q, Chen J, Zhang S, Wang Y, He S and Jia E: Verification of ferroptosis and pyroptosis and identification of PTGS2 as the hub gene in human coronary artery atherosclerosis. Free Radical Biol Med 171: 55-68, 2021.
24. Wang G, Han B, Zhang R, Liu Q, Wang X, Huang X, Liu D, Qiao W, Yang M, Luo X, et al: C1q/TNF-related protein 9 attenuates atherosclerosis by inhibiting hyperglycemia-induced endothelial cell senescence through the AMPKα/KLF4 signaling pathway. Front Pharmacol 12: 758792, 2021.
25. Cui Z, Zhao X, Amevor FK, Du X, Wang Y, Li D, Shu G, Tian Y and Zhao X: Therapeutic application of quercetin in aging-related diseases: SIRT1 as a potential mechanism. Front Immunol 13: 943321, 2022.
26. Meng Q, Xu Y, Ling X, Liu H, Ding S, Wu H, Yan D, Fang X, Li T and Liu Q: Role of ferroptosis-related genes in coronary atherosclerosis and identification of key genes: Integration of bioinformatics analysis and experimental validation. BMC Cardiovasc Dis 22: 339, 2022.

27. Guo Y, Zhang W, Zhou X, Zhao S, Wang J, Guo Y, Liao Y, Lu H, Liu J, Cai Y, *et al*: Roles of ferroptosis in cardiovascular diseases. Front Cardiovasc Med 9: 911564, 2022.

28. Wu D, Hu Q, Wang Y, Jin M, Tao Z and Wan J: Identification of HMOX1 as a Critical Ferroptosis-Related Gene in Atherosclerosis. Front Cardiovasc Med 9: 833642, 2022.

29. Liu H, Xiang C, Wang Z and Song Y: Identification of potential ferroptosis-related biomarkers and immune infiltration in human coronary artery atherosclerosis. Int J Gen Med 15: 2979-2990, 2022.

30. Liu W, Östberg N, Yalcinkaya M, Dou H, Endo-Umeda K, Tang Y, Hou X, Xiao T, Fidler T, Abramowicz S, *et al*: Erythroid lineage Jak2V617F expression promotes atherosclerosis through erythrophagocytosis and macrophage ferroptosis. J Clin Invest 132: e155724, 2022.

31. Yang K, Song H and Yin D: PDSS2 inhibits the ferroptosis of vascular endothelial cells in atherosclerosis by activating Nrf2. J Cardiovasc Pharmacol 77: 767-776, 2021.

32. Bai T, Li M, Liu Y, Qiao Z and Wang Z: Inhibition of ferroptosis alleviates atherosclerosis through attenuating lipid peroxidation and endothelial dysfunction in mouse aortic endothelial cell. Free Radic Biol Med 160: 92-102, 2020.

33. Zhang X, Zhu Y, Zhou Y and Fei B: Interleukin 37 (IL-37) reduces high glucose-induced inflammation, oxidative stress, and apoptosis of podocytes by inhibiting the STAT3-Cyclophilin A (CypA) signaling pathway. Med Sci Monit 26: e922979, 2020.

34. Ruggeri RM, Cristani M, Vicchio TM, Alibrandi A, Giovinazzo S, Saija A, Campennì A, Trimarchi F and Gangemi S: Increased serum interleukin-37 (IL-37) levels correlate with oxidative stress parameters in Hashimoto's thyroiditis. J Endocrinol Invest 42: 199-205, 2019.

35. Chen Y, Luo X, Xu B, Bao X, Jia H and Yu B: Oxidative stress-mediated programmed cell death: A potential therapy target for atherosclerosis. Cardiovasc Drugs Ther 16: 10.1007/s10557-022-07414-z, 2022.

36. Ahmadnia Z, Ranaee M, Abandansari RM, Bagheri N and Shirzad H: Evaluating the MicroRNA expression of IL-35 and IL-37 in helicobacter pylori-infected patients with gastritis and gastric ulcer. Iran J Allergy Asthma Immunol 21: 20-26, 2022.

37. Qin H, Sun C, Zhu Y, Qin Y, Ren S, Wang Z, Li C, Li X, Zhang B, Hao J, *et al*: IL-37 overexpression promotes endometrial regenerative cell-mediated inhibition of cardiac allograft rejection. Stem Cell Res Ther 13: 302, 2022.

38. Cong J, Wu D, Dai H, Ma Y, Liao C, Li L, Ye L and Huang Z: Interleukin-37 exacerbates experimental colitis in an intestinal microbiome-dependent fashion. Theranostics 12: 5204-5219, 2022.

39. Ding Y, Wang Y, Cai Y, Pan C, Yang C, Wang M, Qi X, Ye J, Ji Q, Yu J, *et al*: IL-37 expression in patients with abdominal aortic aneurysm and its role in the necroptosis of vascular smooth muscle cells. Oxid Med Cell Longev 11: 1806513, 2022.

40. Liu T, Liu J, Lin Y, Que B, Chang C, Zhang J, Liang Z, Gao X, Liu S, Liu L, *et al*: IL-37 inhibits the maturation of dendritic cells through the IL-1R8-TLR4-NF-κB pathway. Biochim Biophys Acta Mol Cell Biol Lipids 1864: 1338-1349, 2019.

41. Huang N, Liu K, Liu J, Gao X, Zeng Z, Zhang Y and Chen J: Interleukin-37 alleviates airway inflammation and remodeling in asthma via inhibiting the activation of NF-κB and STAT3 signalings. Int Immunopharmacol 55: 198-204, 2018.

42. Xie M, Tang Q, Nie J, Zhang C, Zhou X, Yu S, Sun J, Cheng X, Dong N, Hu Y and Chen L: BMAL1-downregulation aggravates porphyromonas gingivalis-induced atherosclerosis by encouraging oxidative stress. Circ Res 126: e15-e29, 2020.

43. Wang Z, Liu B, Zhu J, Wang D and Wang Y: Nicotine-mediated autophagy of vascular smooth muscle cell accelerates atherosclerosis via nAChRs/ROS/NF-κB signaling pathway. Atherosclerosis 284: 1-10, 2019.

44. Wei Z, Jing Z, Pinfang K, Chao S and Shaohuan Q: Quercetin inhibits pyroptosis in diabetic cardiomyopathy through the Nrf2 pathway. J Diabetes Res 31: 9723632, 2022.

45. Li MZ, Zhao Y, Dai XY, Talukder M and Li JL: Lycopene ameliorates DEHP exposure-induced renal pyroptosis through the Nrf2/Keap-1/NLRP3/Caspase-1 axis. J Nutr Biochem 113: 109266, 2023.

46. Dodson M, Castro-Portuguez R and Zhang DD: NRF2 plays a critical role in mitigating lipid peroxidation and ferroptosis. Redox Biol 23: 101107, 2019.

47. Dong H, Qiang Z, Chai D, Peng J, Xia Y, Hu R and Jiang H: Nrf2 inhibits ferroptosis and protects against acute lung injury due to intestinal ischemia reperfusion via regulating SLC7A11 and HO-1. Aging 12: 12943-12959, 2020.

48. Wang Y, Yan S, Liu X, Deng F, Wang P, Yang L, Hu L, Huang K and He J: PRMT4 promotes ferroptosis to aggravate doxorubicin-induced cardiomyopathy via inhibition of the Nrf2/GPX4 pathway. Cell Death Differ 29: 1982-1995, 2022.

49. Luo X, Weng X, Bao X, Bai X, Lv Y, Zhang S, Chen Y, Zhao C, Zeng M, Huang J, *et al*: A novel anti-atherosclerotic mechanism of quercetin: Competitive binding to KEAP1 via Arg483 to inhibit macrophage pyroptosis. Redox Biol 57: 102511, 2022.